The linearity and selectivity of neuronal responses in awake visual cortex

Yao Chen Department of Biological Sciences, State University of New York, NY, USA

Sanjiv Anand Department of Biological Sciences, State University of New York, NY, USA

Susana Martinez-Conde Barrow Neurological Institute, Phoenix, AZ, USA

Stephen L. Macknik Barrow Neurological Institute, Phoenix, AZ, USA

Yulia Bereshpolova Department of Psychology, University of Connecticut, Storrs, CT, USA

Harvey A. Swadlow Department of Psychology, University of Connecticut, Storrs, CT, USA

Jose-Manuel Alonso Department of Biological Sciences, State University of New York, NY, USA

Neurons in primary visual cortex (V1) are frequently classified based on their response linearity: the extent to which their visual responses to drifting gratings resemble a linear replica of the stimulus. This classification is supported by the finding that response linearity is bimodally distributed across neurons in area V1 of anesthetized animals. However, recent studies suggest that such bimodal distribution may not reflect two neuronal types but a nonlinear relationship between the membrane potential and the spike output. A main limitation of these previous studies is that they measured response linearity in anesthetized animals, where the distance between the neuronal membrane potential and the spike threshold is artificially increased by anesthesia. Here, we measured V1 response linearity in the awake brain and its correlation with the neuronal spontaneous firing rate, which is related to the distance between membrane potential and threshold. Our results demonstrate that response linearity is bimodally distributed in awake V1 but that it is poorly correlated with spontaneous firing rate. In contrast, the spontaneous firing rate is best correlated to the response selectivity and response latency to stimuli.

Keywords: receptive field, striate cortex, primary visual cortex, thalamocortical, orientation selectivity

Citation: Chen, Y., Anand, S., Martinez-Conde, S., Macknik, S. L., Bereshpolova, Y., Swadlow, H. A., & Alonso, J. (2009). The linearity and selectivity of neuronal responses in awake visual cortex. *Journal of Vision, 9*(9):12, 1–17, http://journalofvision.org/9/9/12/, doi:10.1167/9.9.12.

Introduction

Neurons in the primary visual cortex have been traditionally classified as "simple" and "complex" based on their receptive field properties (Hubel & Wiesel, 1962, 1968). Hubel and Wiesel (1962) classified a cell as "simple" based on four different criteria. First, the receptive field was spatially subdivided into distinct subregions that responded to either light on (on-subregion) or light off (off-subregion). Second, there was spatial summation within each subregion. Third, there was spatial antagonism between on- and off-subregions. And fourth, the visual responses to stationary or moving spots could be predicted from the spatial organization of the subregions (Hubel & Wiesel, 1962). Cells that did not fulfill these four criteria were classified as complex cells. The classification approach proposed by Hubel and Wiesel correlates well with laminar position and synaptic connectivity (Ferster & Lindstrom, 1983; Gilbert, 1977; Hirsch et al., 2002); however, because the criteria are not quantitative, a newer classification method based on measurements of response linearity to drifting gratings has become more frequently used (De Valois, Albrecht, & Thorell, 1982; Movshon, Thompson, & Tolhurst, 1978a, 1978b). This method measures the extent to which the

doi: 10.1167/9.9.12 Received April 8, 2009; published August 25, 2009 ISSN 1534-7362

peristimulus time histogram (PSTH) of a cortical neuron resembles a sinusoid with the same temporal frequency than the drifting grating; that is, a linear replica of the stimulus. By performing a Fourier analysis, the method measures the mean firing rate (F0) and the amplitude of the sinusoid that best fits the PSTH of the cortical neuron (first Fourier harmonic, F1). In linear neurons, the PSTH has a rectified sinusoidal shape, and therefore the amplitude of the first Fourier harmonic (F1) is larger than the mean firing rate (F0). In nonlinear neurons, the PSTH resembles more a step function and the amplitude of F1 is smaller than F0. Two groups of cells typically arise from this analysis with linear cells having F1/F0 ratios >1, nonlinear cells having F1/F0 ratios <1 and F1/F0 been bimodally distributed. Linear cells also tend to have simple receptive fields as defined by Hubel and Wiesel and nonlinear cells tend to have complex receptive fields (De Valois et al., 1982; Movshon et al., 1978b; Schiller, Finlay, & Volman, 1976b; Skottun & Freeman, 1984; Skottun, Grosof, & De Valois, 1988), although classification mismatches between the two methods have been reported (Kagan, Gur, & Snodderly, 2002; Mata & Ringach, 2005; Movshon et al., 1978a; Priebe, Mechler, Carandini, & Ferster, 2004).

The assumption that the bimodality of the F1/F0 distribution represents two types of cells has been recently questioned. Several studies showed, through model and experiment, that a bimodal distribution of F1/F0 in spiking activity could be obtained when F1/F0 was unimodally distributed at the level of the membrane potential (Chance, Nelson, & Abbott, 1999; Mechler & Ringach, 2002; Priebe et al., 2004). To explain this finding, an earlier model proposed that response linearity was directly related to the amount of intracortical excitation that a neuron received; the weaker the intracortical inputs, the stronger the response linearity (Chance et al., 1999). More recently, it has been proposed that the bimodal distribution of response linearity results from the nonlinear relationship between the membrane potential and the spike threshold, which can be seen as another form of intracortical amplification (Mata & Ringach, 2005; Priebe et al., 2004).

Notably, the hypothesis that response linearity depends on the amount of intracortical amplification is based on measurements performed in anesthetized animals, where cortical excitability is reduced by anesthesia. Neurons are likely to be more hyperpolarized and have lower spontaneous firing rates under anesthesia (e.g., Dougherty, Li, Lenz, Rowland, & Mittman, 1997; Zurita, Villa, de Ribaupierre, de Ribaupierre, & Rouiller, 1994); therefore, the response linearity may not be bimodally distributed in the awake brain (Chance et al., 1999; Mata & Ringach, 2005; Priebe et al., 2004). Since the F1/F0 ratio is widely used to classify cortical neurons into two different types, it is important to demonstrate that the bimodal distribution of response linearity is not dependent on an anesthetized state.

Here, we measured a population of V1 neurons in the awake monkey with a median spontaneous firing rate of 6.97 spike/sec, which is approximately 6 times higher than the median reported in recent studies under anesthesia (Ringach, Shapley, & Hawken, 2002; Xing, Ringach, Shapley, & Hawken, 2004). Despite the higher spontaneous activity of our sample, we demonstrate that response linearity is bimodally distributed in the awake V1 cortex, as previously reported under anesthesia. In addition, we demonstrate that the distributions of basic response properties and the correlations among properties are similar in awake and anesthetized animals. Finally, we show that the spontaneous firing rate is correlated with the orientation tuning and response selectivity of the cell but not with response linearity, contrast sensitivity, or receptive field structure. Our results are consistent with the notion that general anesthesia reduces cortical excitability without altering the basic response properties of the V1 neurons. They also support models that associate increased neuronal excitability with a reduction in response selectivity (Chance et al., 1999; Mata & Ringach, 2005; Priebe et al., 2004; but see Ben-Yishai, Bar-Or, & Sompolinsky, 1995; Douglas, Koch, Mahowald, Martin, & Suarez, 1995; Somers, Nelson, & Sur, 1995).

Methods

Data were recorded from two awake, adult rhesus monkeys. All the animal procedures were approved by the Institutional Animal Care and Use Committee (IACUC) at the State University of New York, College of Optometry, and followed the recommendations of the NIH Guide for the Care and Use of Laboratory Animals and the Animal Welfare Act of 1986 and its revisions.

Surgery and behavioral training

Surgery was performed under general anesthesia and sterile conditions in a surgical suite. Each primate underwent two surgeries—first for implantation of a head post and scleral coil and second for implanting the multielectrode array. Each surgery was followed by a period of recovery of about 2 weeks, after which the animal was trained to perform visual fixation. After the first surgery, the primates learned to fixate a small cross (0.1 degree) that was presented on the screen when they grabbed a bar. Then, they learned to maintain visual fixation within 0.5–1 degrees of the cross and to release the bar for reward after detecting a color change in one of 5 gratings presented peripherally. Once the animals were trained to fixate, the second surgery to implant the electrodes was performed. During the second surgery, a craniotomy was performed overlying the striate cortex (V1) within the recording chamber. A multielectrode array was placed within the recording chamber, above the brain, in a region without

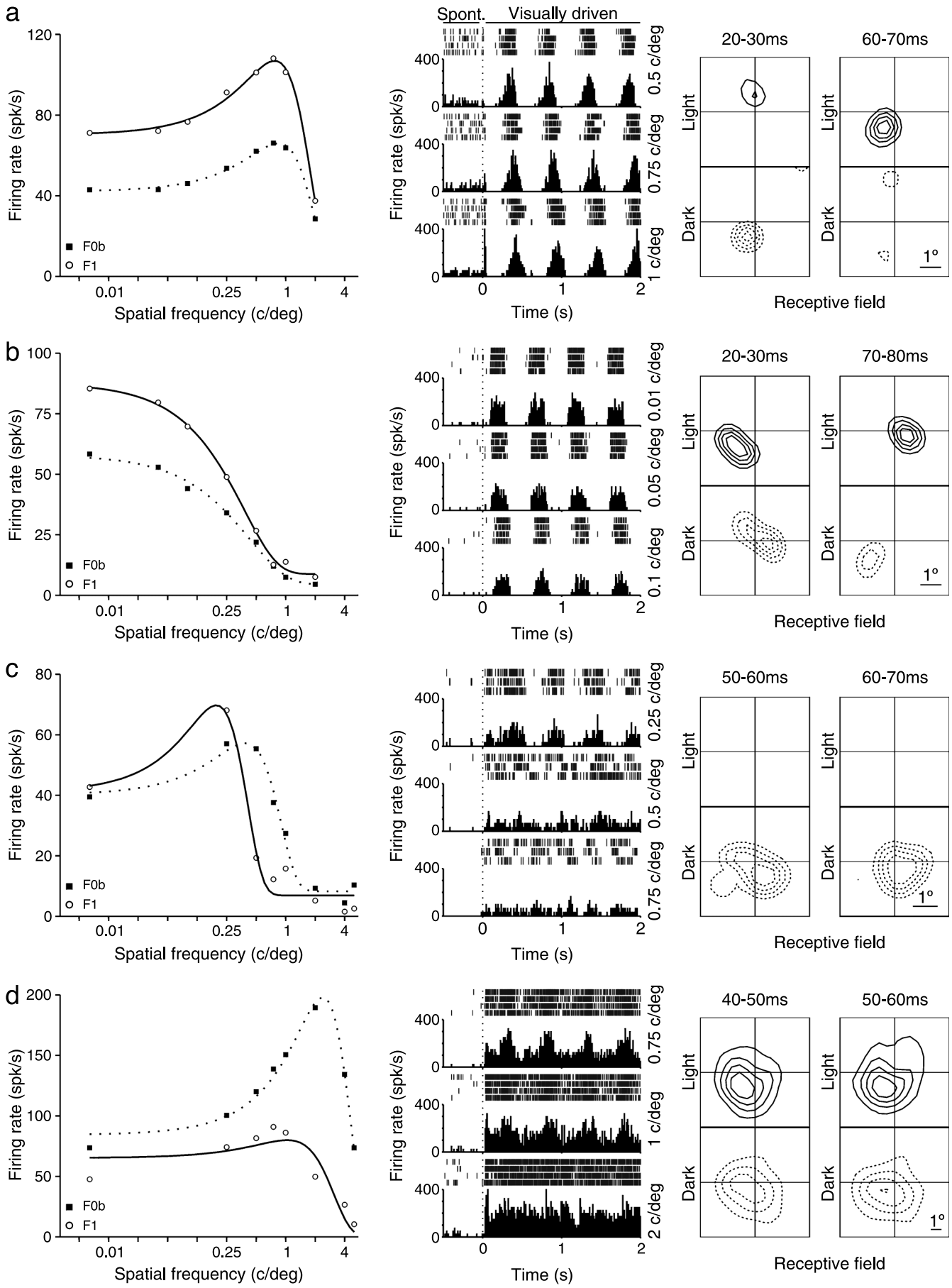
a
b
c
d
Firing rate (spk/s)
Spatial frequency (c/deg)
F0b
F1
Spont.
Visually driven
0.5 c/deg
0.75 c/deg
1 c/deg
0.01 c/deg
0.05 c/deg
0.1 c/deg
0.25 c/deg
2 c/deg
Time (s)
20-30ms
60-70ms
70-80ms
50-60ms
40-50ms
Light
Dark
1°
Receptive field

large superficial blood vessels. Each primate was implanted with an array of 3–7 independently movable electrodes, organized in a triangular or concentric array, and separated by 150 to 400 microns. (Swadlow, Bereshpolova, Bezdudnaya, Cano, & Stoelzel, 2005) and each multielectrode array remained implanted in the brain for 6 months to over 1 year. During this time, the interior of the recording chamber remained sealed. After placing the multielectrode array, the craniotomy was covered with antibiotic ointment and the multielectrode array was attached to the bone with bone cement.

Visual stimuli and electrophysiological recording

Visual stimuli were generated with a computer running Visionworks (Vision Research Graphics, Inc.) and presented on a GDM-F520 monitor (SONY Electronics Inc., USA; 160 Hz). Stimuli for reverse correlation analysis were generated with a different computer (custom software from Swadlow's laboratory) and presented on the same monitor at 100 Hz. Another computer running Rasputin (Plexon Corp., Dallas, TX) was used for data acquisition. Eye movements were recorded at 5,000 Hz and cortical spikes at 40,000 Hz. Cortical spikes were recorded with the chronically implanted multielectrode array, which allowed us to move each electrode independently. Because the electrodes are sharp, ultrathin (1 micron at the tip, 40 microns at the shaft) and they are attached to microdrives that are fixed to the skull, we were able to record well-isolated units and the recordings were very stable. Cells selected for this study had eccentricities that ranged between 5° and 21°. All the visual stimulation presented in this paper was binocular.

Each cell was first carefully mapped to identify the optimal stimulus parameters that generated the strongest response (grating patch location, size, orientation, temporal frequency, and spatial frequency). To quantify the spatial frequency tuning, visual responses were measured with 8 different spatial frequencies that most commonly ranged between 0.01 and 2 cycles per degree and occasionally between 0.01–5 and 0.25–5 cycles per degree. For quantifying orientation, we used drifting gratings moving at 16 different directions and 8 different orientations. All gratings were presented at a temporal frequency that was fixed for each cell (usually 2–3Hz). A blank image of uniform luminance was shown 400 msec before the beginning of the stimulus, and this time period was used to calculate the spontaneous firing rate of each cell.

Data analysis

Response linearity and spatial frequency

Response linearity (F1/F0): The response linearity was calculated from the visual responses to drifting gratings presented at different spatial frequencies. The visual response was quantified from peristimulus time histograms (PSTHs) obtained with 10-msec time bins over a time period of 1.8 sec (we discarded the initial 0.2 sec to eliminate the response to the stimulus onset). We used Fourier analysis to measure the amplitude of the first harmonic (F1) and mean firing rate (F0) from PSTHs obtained for each spatial frequency tested (both F1 and F0 have units of spikes/second). This procedure is equivalent to fitting a sinusoid to the PSTH (with the same temporal frequency of the drifting grating) to obtain F1 and then averaging the firing rate across the entire drifting grating stimulation to obtain F0.

The original studies that described the measurements of response linearity obtained F0 by subtracting the spontaneous firing rate from the mean firing rate under visual stimulation (De Valois et al., 1982; Movshon et al., 1978a, 1978b; Skottun et al., 1991). To be consistent with the terminology from these original studies, here we use the term F0 if the mean firing rate was measured after subtracting the spontaneous firing rate, and we use F0b if the mean firing rate was obtained directly from the PSTH (the original F0 term plus baseline). Probably because the V1 spontaneous activity is higher in the awake state than under anesthesia, F1/F0 was not bimodally distributed when F0 was obtained as in the original studies (p = 0.5009, Hartigan test). However, a significant bimodal distribution was obtained if the spontaneous firing rate was subtracted directly from the PSTH (p = 0.039, Hartigan test; Figure 2d). That is, the PSTH

Figure 1. Examples of four cells recorded in the awake primary visual cortex. Left panels show F1 and F0b responses of individual cells stimulated with drifting gratings at different spatial frequencies (for definition of F0b, see Methods). Middle panel shows rasters and PSTHs obtained for three selected spatial frequencies while the monkeys were fixating, 500 msec before the presentation of the drifting grating, and during 2 sec of visual stimulation with drifting gratings. The dotted line marks the stimulus onset; the spontaneous activity was measured within 400 msec before the dotted line. Right panels show the receptive field of each cell obtained by reverse correlation under stimulation with light and dark squares (shown at two different time windows). (a) Cell that generated linear responses (F1 > F0b) across all spatial frequencies (left) and had high spontaneous firing rate (middle) and a receptive field with small, transient, round on- and off-subregions. (b) Cell that generated linear responses (F1 > F0b) across all spatial frequencies (left) and had low spontaneous firing rate (middle) and a receptive field with elongated, transient on- and off-subregions. (c) Cell that generated linear responses (F1 > F0b) at low spatial frequencies and nonlinear responses (F0b > F1) at high spatial frequencies (left) and had low spontaneous firing rate (middle) and an off-sustained receptive-field (unlike the transient receptive fields shown above, this receptive field did not reverse sign at 50–60 msec). (d) Cell that generated nonlinear responses (F0b > F1) across all spatial frequencies and had low spontaneous firing rate (middle) and a sustained on/off receptive field.

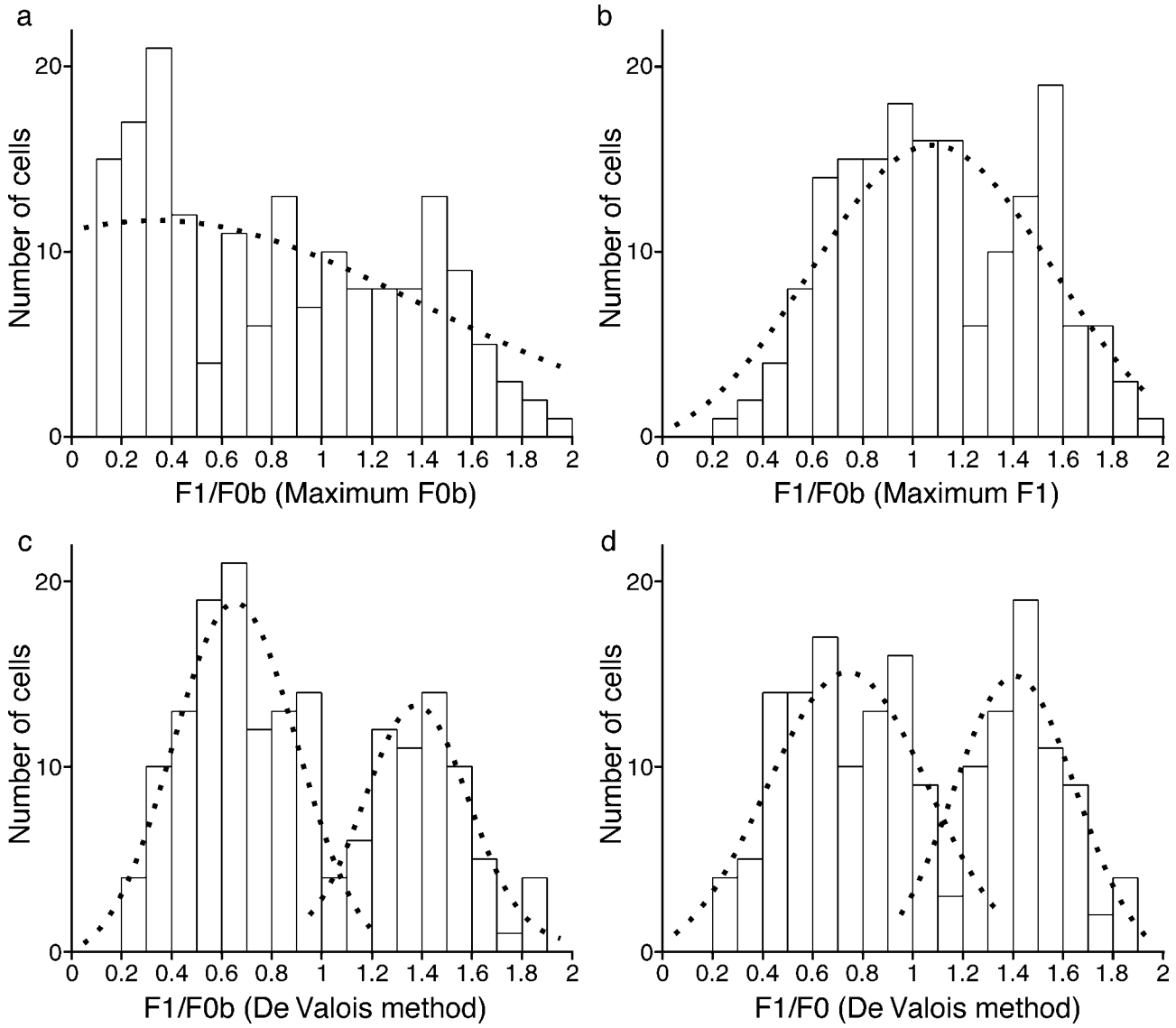

Figure 2. Distribution of response linearity (F1/F0) fitted with Gaussian functions (dotted line) and computed by four different methods. (a) F1/F0b measured at the spatial frequency that generated the maximum F0b response. (b) F1/F0b measured at the spatial frequency that generated the maximum F1 response. (c) F1/F0b measured as an average of F1 and F0b over the three spatial frequencies that generated the largest combined F1 and F0b responses. (d) Same as panel c but after subtracting the spontaneous firing rate.

was rectified by a constant value equal to the mean spontaneous activity, and then we calculated F1 and F0 from the rectified PSTH. Therefore, in this paper, F0b is the mean firing rate under visual stimulation and F0 is the mean firing rate minus the spontaneous activity obtained by rectifying the PSTH. In neurons with PSTHs resembling a sinusoid, like neurons in Figures 1b and 1c, F1 was larger than F0b because the amplitude of the sinusoid was larger than the mean firing rate. In neurons with PSTHs resembling a step function, like the neuron in Figure 1d, F0b > F1 because the amplitude of the sinusoid fitted to the PSTH was small in comparison to the mean firing rate.

Since the strongest F1 and F0b responses were not always generated at the same spatial frequency, the F1/F0b ratio was also measured using a procedure originally described by De Valois et al. (1982). First, we selected the three spatial frequencies that generated the largest combined F1 and F0b responses. Then, we obtained an F1 average and an F0b average and calculated the F1/F0b ratio from these two average values. Cells were classified as "linear" and "nonlinear" based on the F1/F0b ratio. Therefore, the F1/F0 ratio was plotted based on four different criteria. In the first method, we measured the F1/F0b at the spatial frequency that generated the maximum F0b response. In the second method, we measured F1/F0b at spatial frequency that generated the maximum F1 response. In the third method, F1/F0b was computed at the three spatial frequencies that generated the largest combined F1 and F0b responses, as originally described by De Valois et al.

Finally, in the fourth method, F1/F0 was computed as in the third but after subtracting the spontaneous activity. Each of the distributions was fitted with single and double Gaussian functions and the goodness of the fits (r^2) were calculated. For distributions fitted with two Gaussian functions, we divided the F1/F0 distribution into two groups (first group with F1/F0 < 1 and second group with F1/F0 > 1) and then we calculated the average r^2 value. Significant differences between single- and double-Gaussian fits were calculated by performing a bootstrap analysis to obtain 20 r^2 values per fit and then comparing the r^2 values from single and double Gaussian fits with a Mann–Whitney test. The distribution of F1/F0 ratios was also tested for bimodality with the Hartigan test (Hartigan & Hartigan, 1985).

Spatial frequency: The spatial frequency tuning curves were fitted with Gaussian functions, and these functions were used to extract the spatial frequency peak, defined as the spatial frequency that elicited maximum response. For each cell, we also selected the half of the spatial frequency tuning curve that had the overall strongest response and defined spatial frequency half-bandwidth as the half width at half height of the tuning curve.

Orientation tuning and direction selectivity

To quantify orientation tuning, we measured the circular variance (Ringach, Shapley, et al., 2002). The circular variance was defined as CV = 1 − |*R*|, where *R* is:

$$R = \frac{\sum_k r_k^{e^{i2\theta_k}}}{\sum_k r_k}, \quad (1)$$

r_k is the mean spike rate in response to a drifting grating and θ_k the angle of the drifting grating expressed in radians. The values of circular variance range from 0 to 1. Cells with sharp orientation tuning have values of circular variance close to zero and those with broad orientation tuning have values close to one. The direction selectivity (DS) was measured at the preferred orientation of the cell as DS = 1 − R_{NPD}/R_{PD}, where R_{PD} and R_{NPD} are the neuronal responses to gratings moving in preferred and nonpreferred direction. A neuron was classified as directional selective if the direction selectivity exceeded 0.5.

Response selectivity

We calculated the selectivity of a neuron to visual stimuli, response selectivity (*S*), as: *S* = 1 − ((CV + (1 − DS) + SFs) / 3), where CV is circular variance (CV), DS is direction selectivity, and SFs is spatial frequency selectivity. The spatial frequency selectivity was calculated as (SFw / maximum SFw in the total cell population), where SFw is the spatial frequency half-bandwidth (in octaves) obtained from the spatial frequency tuning. The values of response selectivity also ranged from 0 to 1. Cells that were very selective for orientation tuning (sharp tuning), direction (stronger response to preferred direction than the opposite), and spatial frequency tuning (sharp tuning) had values close to 1 and those that were not selective had values closer to 0.

Correlation between F1 and F1/F0

We used the power law from Priebe et al. (2004) to estimate the correlation between the F0b amplitude and the F1/F0b ratio that would be expected from a model where the bimodality of F1/F0b ratios at the spike output results from a unimodal distribution of F1/F0b ratios at the membrane potential. The relationship between membrane potential and firing rate was calculated as follows:

$$R(V_m) = k[V_m - V_{rest}]_+^p, \quad (2)$$

where V_m is the membrane potential, V_{rest} is the resting membrane potential (taken from response from a blank stimulus), *k* is the gain factor, and *p* is the exponent. The subscript "+" indicates rectification (i.e., that values below zero are set to zero; Priebe et al., 2004). We used the values of firing rate to obtain F1 and F0b values and plot the expected relationship between F1 and F1/F0b (see Figure 3a). Note that the equation from Priebe et al. (2004) is similar to the equation from Mechler and Ringach (2002) to model the F1/F0b distribution. We chose the equation from Priebe et al. because it uses the resting potential as a parameter.

Receptive field structure and response latency

The receptive field structure was measured in 124 V1 neurons by reverse correlation with sparse noise (Jones & Palmer, 1987). The sparse noise consisted of small light and dark squares (0.2–0.4 degrees/side) presented for 40 msec in a gray background. ON and OFF receptive field maps were obtained from the neuronal responses to light and dark spots, respectively. We used different time windows (10-msec bins from 0 to 100 msec) and smoothed each receptive field map with a Gaussian filter (sigma 0.2–0.4 degrees). Examples of ON and OFF maps are illustrated in Figure 1.

We measured "on" and "off" subregions (R_{ON} and R_{OFF}) in each receptive field map at time windows where the visual response was significantly different from noise (>3 times the noise standard deviation, *n* = 108). Neurons that responded poorly to sparse noise were not included in this analysis (*n* = 16). We calculated the spatial relationship between R_{ON} and R_{OFF} by performing five different measurements, as in (Mata & Ringach, 2005): discreteness, correlation coefficient, normalized distance, overlap index, and relative phase. The *discreteness* was computed

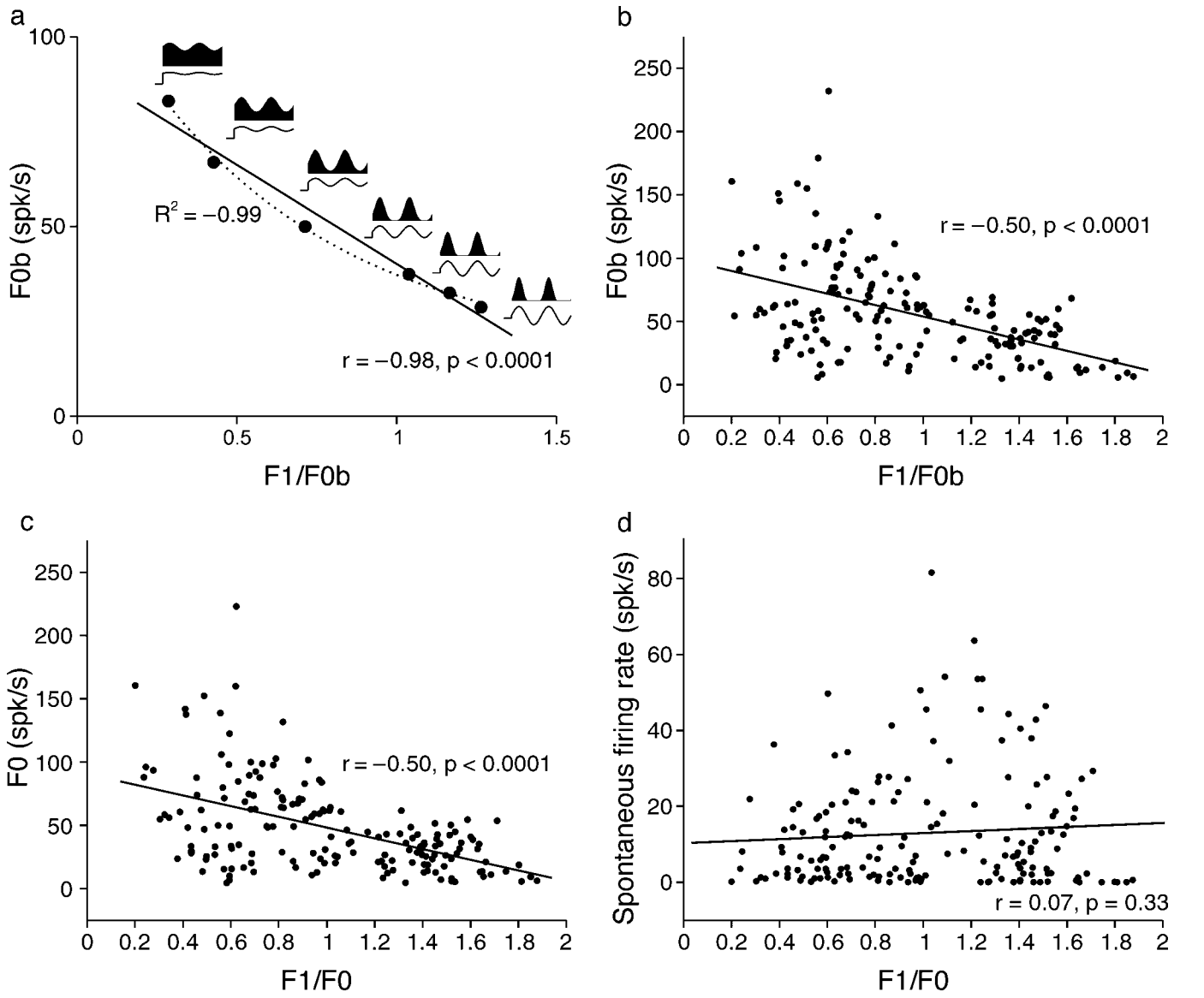

Figure 3. Relationship between F1/F0 ratio and mean firing rate (F0) and between F1/F0 ratio and spontaneous activity. (a) Simulated plot of F0b against F1/F0b obtained by using the power law described by Priebe et al. (2004). (b) Plot of F0b against F1/F0b measured in the awake primary visual cortex (De Valois et al. method without subtracting spontaneous activity). (c) Plot of F0 against F1/F0 measured in the awake primary visual cortex (De Valois et al. method after subtracting spontaneous activity). (d) Plot of spontaneous firing rate against F1/F0. The solid line in each plot represents the linear regression.

as $\Sigma|R_{ON} - R_{OFF}| / (\Sigma|R_{ON}| + \Sigma|R_{OFF}|)$, and it is ≈0 for complex cells and ≈1 for simple cells (Dean & Tolhurst, 1983). The *correlation coefficient* was computed as the correlation between R_{ON} and R_{OFF}, which is ≈+1 for complex cells and ≈−1 for simple cells. The *normalized distance* was computed as the distance between the center of R_{ON} and R_{OFF} divided by the average of the square roots of the R_{ON} and R_{OFF} areas, which is ≈0 for complex cells and »0 for simple cells. The *overlap index* was computed as $((\sigma_{ON} + \sigma_{OFF}) - |m_{ON} - m_{OFF}|) / ((\sigma_{ON} + \sigma_{OFF}) + |m_{ON} - m_{OFF}|)$, where σ_{ON} σ_{OFF} and m_{ON} m_{OFF} are the standard deviations, and means of Gaussian functions fitted to P_{ON} and P_{OFF} and P_{ON} and P_{OFF} are 1D receptive field slices performed at the centers of R_{ON} and R_{OFF}. The overlap index is ≈1 for complex cells and <1 for simple cells (Schiller, Finlay, & Volman, 1976a). The *relative phase* was computed as $\Delta\Phi = |\Phi_{ON} - \Phi_{OFF}|$, where Φ_{ON} Φ_{OFF} are the phases of Gabor functions fitted to P_{ON} and P_{OFF}, which is ≈0 for complex cells and ≈π for simple cells (Conway & Livingstone, 2003). Measurements of overlap index and relative phase were only performed in neurons that responded robustly to both light and dark stimuli (n = 63).

The receptive field maps obtained by reverse correlation were also used to measure the response latency of each cell. The response latency was measured at the 10-msec

time window that showed the earliest significant visual response. Then, the upper limit of this window was progressively reduced in steps of 1 msec until the response was no longer significant. The upper limit of the narrowest temporal window with significant response was chosen as the value of response latency.

Results

We recorded from 173 cells in primary visual cortex from two awake rhesus monkeys (*Macaca mulatta*) and measured their response linearity, spontaneous firing rate, and receptive field properties. To be consistent with terminology used in previous studies (De Valois et al., 1982; Movshon et al., 1978a, 1978b; Skottun et al., 1991), we call F0 the mean rate under visual stimulation minus the spontaneous activity and we call F0b the mean rate under visual stimulation without any subtraction (the original F0 term plus "baseline"; for details, see Methods). Figure 1 shows representative examples of four cells. The cell in Figure 1a generated linear responses to drifting gratings (F1 > F0b) for all spatial frequencies tested (Figure 1a, left) and had high spontaneous activity (29 spikes/sec; Figure 1a, middle) and a receptive field with a small, round, off-subregion and a weaker, round on-subregion (Figure 1a, right). The cell in Figure 1b was also linear across all spatial frequencies tested (Figure 1b, left) and had low spontaneous activity (3 spikes/sec; Figure 1b, middle), and the receptive field had separate and elongated on- and off-subregions (Figure 1b, right). The cell in Figure 1c was linear when tested at low spatial frequencies but not at high spatial frequencies (Figure 1c, left); the spontaneous activity was low (2 spikes/sec; Figure 1c, middle), it responded only to dark spots and the response was sustained over several tens of milliseconds (Figure 1c, right). Cells that generate linear responses at some spatial frequencies but not others were originally described in the anesthetized primate by De Valois et al. (1982, see below), and a more recent paper (Priebe et al., 2004) in the cat illustrates a cell with remarkably similar tuning to the one illustrated here (Figure 5c in Priebe et al., 2004). Finally, Figure 1d shows a cell that generated nonlinear responses across all spatial frequencies tested (Figure 1d, left) and had low spontaneous firing rate (7 spikes/sec; Figure 1d, middle) and a receptive field that generated on–off sustained responses (Figure 1d, right). If the four Hubel and Wiesel criteria were applied, the cells illustrated in Figures 1a and 1b would be classified as simple and the cells in Figures 1c and 1d as complex cells.

The first question that we addressed was whether the F1/F0 ratios were bimodally distributed across V1 neurons in the awake primate. To our knowledge, a bimodal distribution of F1/F0 has only been demonstrated in anesthetized animals (see Table 1). While the F1/F0 ratio is a widely used method to measure response linearity and classify cells in primary visual cortex, the method to measure F1 and F0 varies considerably across laboratories. The first source of ambiguity is raised by cells like the one illustrated in Figure 1c. This cell would be classified as linear if measured at the spatial frequency that generated the maximum F1 response and nonlinear if measured at the spatial frequency that generated the maximum F0b response.

Here, we used four different methods to calculate the distribution of F1/F0. First, we calculated the F1/F0b ratios by making the measurements of F1 and F0b at the spatial frequency that generated the maximum F0b (Figure 2a). This distribution was relatively flat, was poorly fitted with either one or two independent Gaussian functions (r^2 for two-Gaussians = 0.45; r^2 for one Gaussian = 0.23), and was not significantly bimodal (p = 0.93, Hartigan test). The second approach was to make the F1/F0b measurements at the spatial frequency that generated the maximum F1 (Figure 2b). Again, the difference between one- and two-Gaussian fits was not significant with two different Gaussians than a single Gaussian function, but the difference was not significant (r^2 = 0.6 versus r^2 = 0.66, difference = 0.06, p = 0.08, Bootstrap and Mann–Whitney test). A Hartigan test for bimodality did not reach significance either (p = 0.21). The third method was the one original described by De Valois et al. (1982). De Valois et al. noticed the existence of cells like the one illustrated in Figure 1c and was aware of the problem that these cells caused when measuring response linearity. To address this problem, De Valois et al. proposed to select the three spatial frequencies that generate the strongest combined F1 and F0 responses and then calculate the F1/F0 ratios as the average F1/average F0 obtained from the three selected spatial frequencies. The distribution obtained with the De Valois et al. method was better fitted with two different Gaussians than a single Gaussian function (r^2 = 0.79 versus r^2 = 0.47, difference = 0.32, $p < 0.0001$, Bootstrap and Mann–Whitney test) and also reached significance with a Hartigan test (p = 0.017). The fourth method was to repeat the De Valois et al. method, including the subtraction of the spontaneous activity. The average spontaneous activity in our sample was 12.87 spikes/sec with a median of 6.97 spikes/sec. The subtraction of the spontaneous activity slightly shifted the distribution toward the linear side without altering its general shape. This distribution was also better fitted with two Gaussians than a single Gaussian (r^2 = 0.72 versus r^2 = 0.46, difference = 0.26; $p < 0.0001$, Bootstrap and Mann–Whitney test) and also reached significance with a Hartigan test (p = 0.039). As shown in this figure (see also Figure 3), the subtraction of spontaneous activity had a minor effect on the distribution of F1/F0; therefore, in most of the figures of this paper, we use F0b instead.

Previous studies (Mechler & Ringach, 2002; Priebe et al., 2004) demonstrated that it is possible to obtain a

Reference	Used F1/F0 ratio to classify cortical cells	Animal	*N*	Showed distribution of F1/F0 ratios	Showed statistically significant bimodality
Schiller et al. (1976b)	Yes	M	86	Yes	Not tested
Movshon et al. (1978a)	Yes	C	164	No	Not tested
Dean (1981)	Yes	C	43	No	Not tested
De Valois et al. (1982)	Yes	M	343	Yes	Not tested
Dean and Tolhurst (1983)	Yes	C	563	Yes	Not tested
Skottun, Bradley, Sclar, Ohzawa, and Freeman (1987)	Yes	C	48	No	Not tested
Lennie, Krauskopf, and Sclar (1990)	Yes	M	171	No	Not tested
Skottun et al. (1991)	Yes	C	1061*	Yes	Not tested
Casanova, Nordmann, Ohzawa, and Freeman (1992)	Yes	C	176	No	Not tested
DeAngelis, Freeman, and Ohzawa (1994)	Yes	C	82	No	Not tested
Chino, Smith, Yoshida, Cheng, and Hamamoto (1994)	Yes	C	89	No	Not tested
Hawken, Shapley, and Grosof (1996)	Yes	M	75	No	Not tested
Hawken et al. (1996); Ohzawa, DeAngelis, and Freeman (1996, 1997)	Yes	C	109	No	Not tested
Smith, Chino, Ni, Ridder, and Crawford (1997)	Yes	M	239	No	Not tested
Cumming, Thomas, Parker, and Hawken (1999)	Yes	M	336	Yes	Not tested
Sceniak, Ringach, Hawken, and Shapley (1999)	Yes	M	85	No	Not tested
Ringach, Shapley, et al. (2002)	Yes	M	308	Yes	Yes
Kagan et al. (2002)	Yes	M	114	Yes	No
Priebe et al. (2004)	Yes	C	102	Yes	Yes
Ibbotson, Price, and Crowder (2005)	Yes	W	123	Yes	Yes
Mata and Ringach (2005)	Yes	M	98	Yes	No

Table 1. Examples of studies which used response linearity (F1/F0) to classify cortical cells. M = Monkey; C = Cat; W = Wallaby; *N* = sample size. *Note*: *Data combined from five laboratories.

bimodal distribution of F1/F0 ratios from the spike output when the distribution is unimodal at the level of the membrane potential. In these studies, the bimodal distribution results from the nonlinear relationship between membrane potential and spiking activity, and this relation can be accurately described by a power law. The power law described by Priebe et al. (2004) predicts a strong correlation between the mean firing rate (F0b) and the F1/F0b ratio (Figure 3a) that can be fit with a linear ($r = -0.98$, $p < 0.0001$) and an exponential function ($r^2 = 0.99$, $Y = 16.1 + 103.9e^{-1.6X}$).

A significant linear relation between F0b and F1/F0b ratio could be demonstrated in the awake primate when F1/F0 was calculated using the De Valois et al. method without (Figure 3b) or with subtraction of spontaneous activity (Figure 3c). However, the correlation was weaker ($r = -0.5$, $p < 0.0001$) than that described by a single exponential function. The two main reasons for the weak correlation were the diversity of PSTH shapes and the wide range of firing rates, particularly for cells with F1/F0 < 1. For example, the two cells with F1/F0 < 1 illustrated in Figure 1 had mean firing rates of ~200 spikes/sec (e.g., Figure 1d) and <50 spikes/sec (Figure 1c). Moreover, there were some color-selective cells with F1/F0 < 1 that responded poorly to luminance gratings. The weak correlation between F0 and F1/F0 could result from a combination of multiple power laws with different exponents. The different exponents may reflect the diversity of nonlinear relations between membrane potential and spiking output across cells in visual cortex (Priebe et al., 2004).

The F1/F0 ratio was weakly correlated with the spontaneous firing rate of the cell ($r = -0.14$, $p = 0.06$; Figure 3d), as would be expected from the relatively similar spike thresholds and mean membrane potentials of linear and nonlinear cells measured in cat visual cortex (Priebe et al., 2004). Stronger correlations could be demonstrated between the spontaneous firing rate and other response properties. Figure 4 shows multiple correlations between spontaneous firing rate and several response properties including selectivity to orientation, spatial frequency, and direction of movement, measured individually or combined. It also shows correlations with

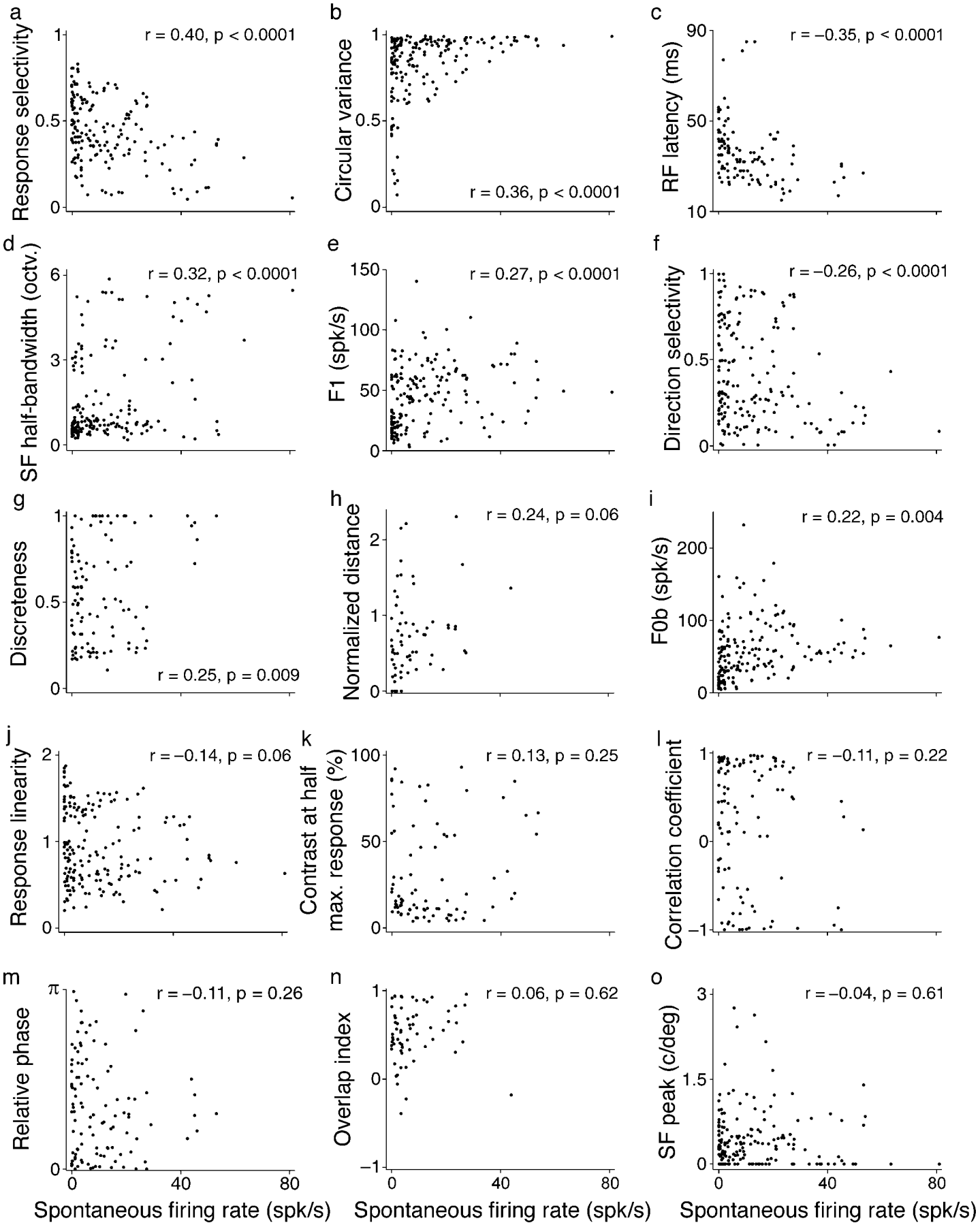
a
Response selectivity
r = 0.40, p < 0.0001
b
Circular variance
r = 0.36, p < 0.0001
c
RF latency (ms)
r = −0.35, p < 0.0001
d
SF half-bandwidth (octv.)
r = 0.32, p < 0.0001
e
F1 (spk/s)
r = 0.27, p < 0.0001
f
Direction selectivity
r = −0.26, p < 0.0001
g
Discreteness
r = 0.25, p = 0.009
h
Normalized distance
r = 0.24, p = 0.06
i
F0b (spk/s)
r = 0.22, p = 0.004
j
Response linearity
r = −0.14, p = 0.06
k
Contrast at half max. response (%)
r = 0.13, p = 0.25
l
Correlation coefficient
r = −0.11, p = 0.22
m
Relative phase
r = −0.11, p = 0.26
n
Overlap index
r = 0.06, p = 0.62
o
SF peak (c/deg)
r = −0.04, p = 0.61
Spontaneous firing rate (spk/s)
Spontaneous firing rate (spk/s)
Spontaneous firing rate (spk/s)

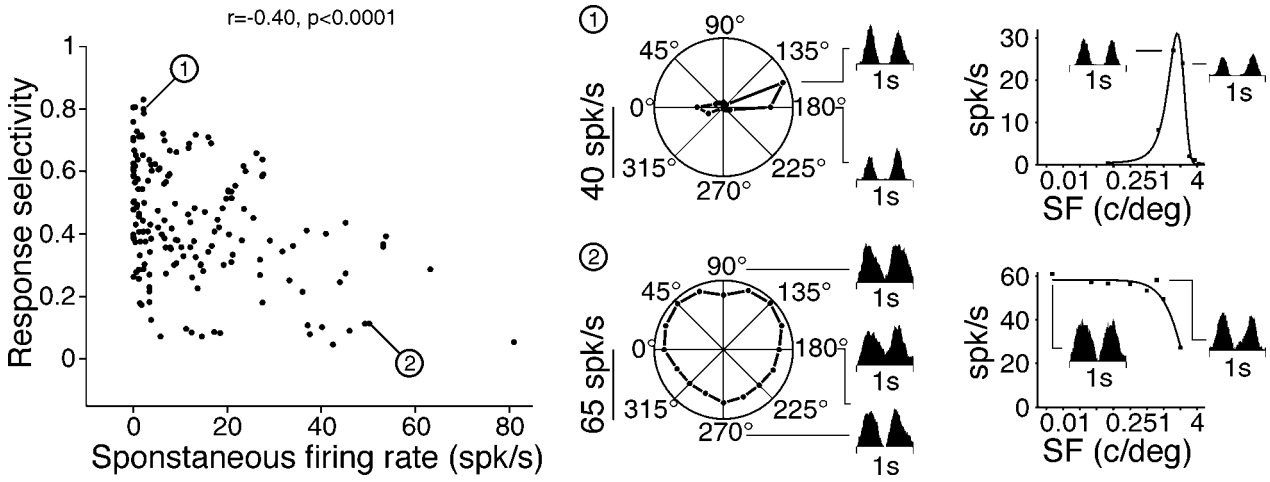

Figure 5. Relationship between spontaneous firing rate and response selectivity. The orientation/direction and spatial frequency selectivity are shown on the right for two cell examples (1, 2).

contrast sensitivity, response amplitude (F1 or F0b), and receptive field structure. The receptive field structure was measured using five different methods that quantify the overlap/distance between on and off receptive field subregions, as in Mata and Ringach (2005).

The spontaneous firing rate was most strongly correlated with the response selectivity to stimuli ($r = 0.4$, $p < 0.0001$), the orientation tuning ($r = 0.36$, $p < 0.0001$), and the response latency of the cell ($r = -0.35$, $p < 0.0001$). The negative correlation between the spontaneous firing rate and the response latency is particularly interesting because it replicates, at the level of V1, a trend that is observed in the early visual pathway: a reduction in spontaneous activity as information progresses from retina to thalamus and from thalamus to visual cortex. The relation between spontaneous firing rate and response selectivity is also important because it provides support to models that associate high cortical amplification to a loss of response selectivity (Chance et al., 1999; Mata & Ringach, 2005; Priebe et al., 2004).

The relation between spontaneous firing rate and orientation tuning (Figure 4b) has been previously demonstrated in the anesthetized primate (Ringach, Shapley, et al., 2002; Xing et al., 2004). This relation can be fit with a linear equation ($r = 0.36$, $p < 0.0001$) but it is clearly best described by a triangular space than by a straight line. The scatter plot in Figure 4b shows a triangular distribution so that the cells with the highest spontaneous activity (>30 Hz) had all poor orientation selectivity and cells with the sharpest orientation tuning (circular variance <0.3) had all very low spontaneous activity. This relation can still be demonstrated after subtracting the spontaneous firing rate in the calculation of circular variance (not shown, $r = 0.28$, $p < 0.0001$).

The relation between spontaneous firing rate and response selectivity, the strongest correlation from Figure 4, is illustrated with specific cell examples in Figure 5. The response selectivity has a value of 1 in cells with high direction selectivity and narrow tuning (orientation and spatial frequency) and zero in cells with no direction selectivity and broad tuning. This relationship has also a triangular shape. The most selective cells (selectivity >0.8) tended to have low spontaneous firing rates and the cells with highest spontaneous activity (>40 spikes/sec) tended to have low selectivity to stimuli.

We have shown that at least the bimodal distribution of response linearity and the correlation between circular variance and spontaneous firing in V1 do not seem to differ substantially between anesthetized and awake primates. However, it is possible that other basic response properties may change under anesthesia. To address this possibility, we replicated the detailed measurements performed by Mata and Ringach (2005) on the receptive field structure of V1 neurons in the anesthetized primate. Mata and Ringach measured the relation between on and off receptive field regions of single V1 neurons by using

Figure 4. Relationship between the spontaneous firing rate and the cell response properties. (a) Combined selectivity to orientation, spatial frequency, and direction of motion (0 = nonselective, 1 = very selective). (b) Orientation tuning measured as circular variance (0 = sharp tuning, 1 = broad tuning). (c) Receptive field latency measured by reverse correlation. (d) Spatial frequency tuning measured as half-width at half-height (octaves). (e) Response amplitude measured as the first Fourier harmonic of the PSTH. (f) Directional selectivity (0 = nondirectional, 1 = very directional). (g) Measurement of on/off overlap (0 = no overlap, 1 = high overlap). (h) Measurement of on/off overlap (0 = high overlap, >0 = increasingly less overlap). (i) Response amplitude measured as the mean firing rate. (j) F1/F0b. (k) Contrast that generated half of the maximum response. (l) Measurement of on/off overlap (−1 = no overlap, +1 = high overlap). (m) Measurement of on/off overlap (0 = overlap, π = no overlap). (n) Measurement of on/off overlap (<1 = increasingly less overlap, 1 = overlap). (o) Peak of spatial frequency tuning.

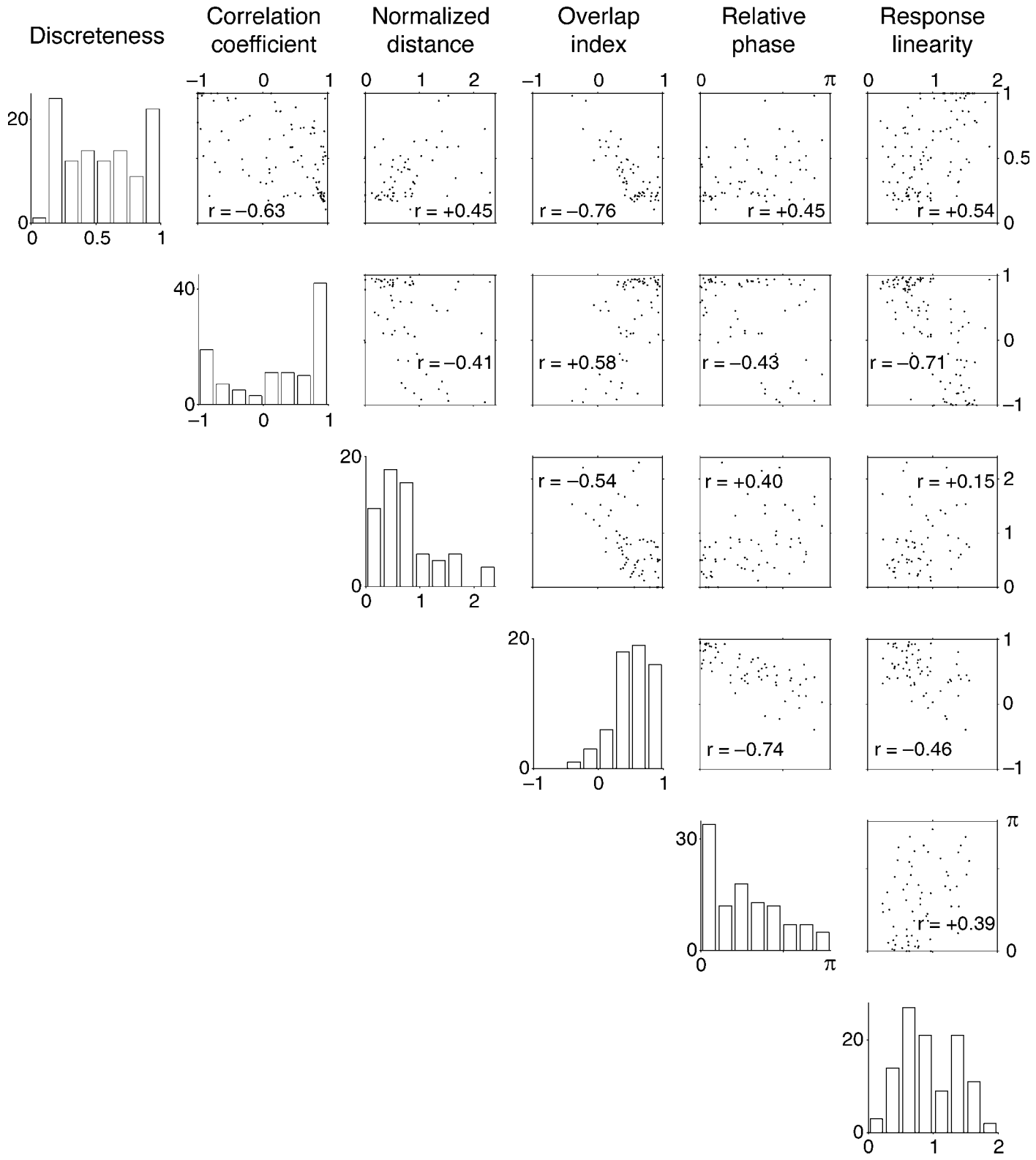

Figure 6. Correlations between five different measurements of receptive field structure and response linearity. The distributions and correlations measured in awake primate V1 are similar to those measured by Mata and Ringach (2005) in the anesthetized primate V1. See Methods for definition of discreteness, correlation coefficient, normalized distance, overlap index, and relative phase.

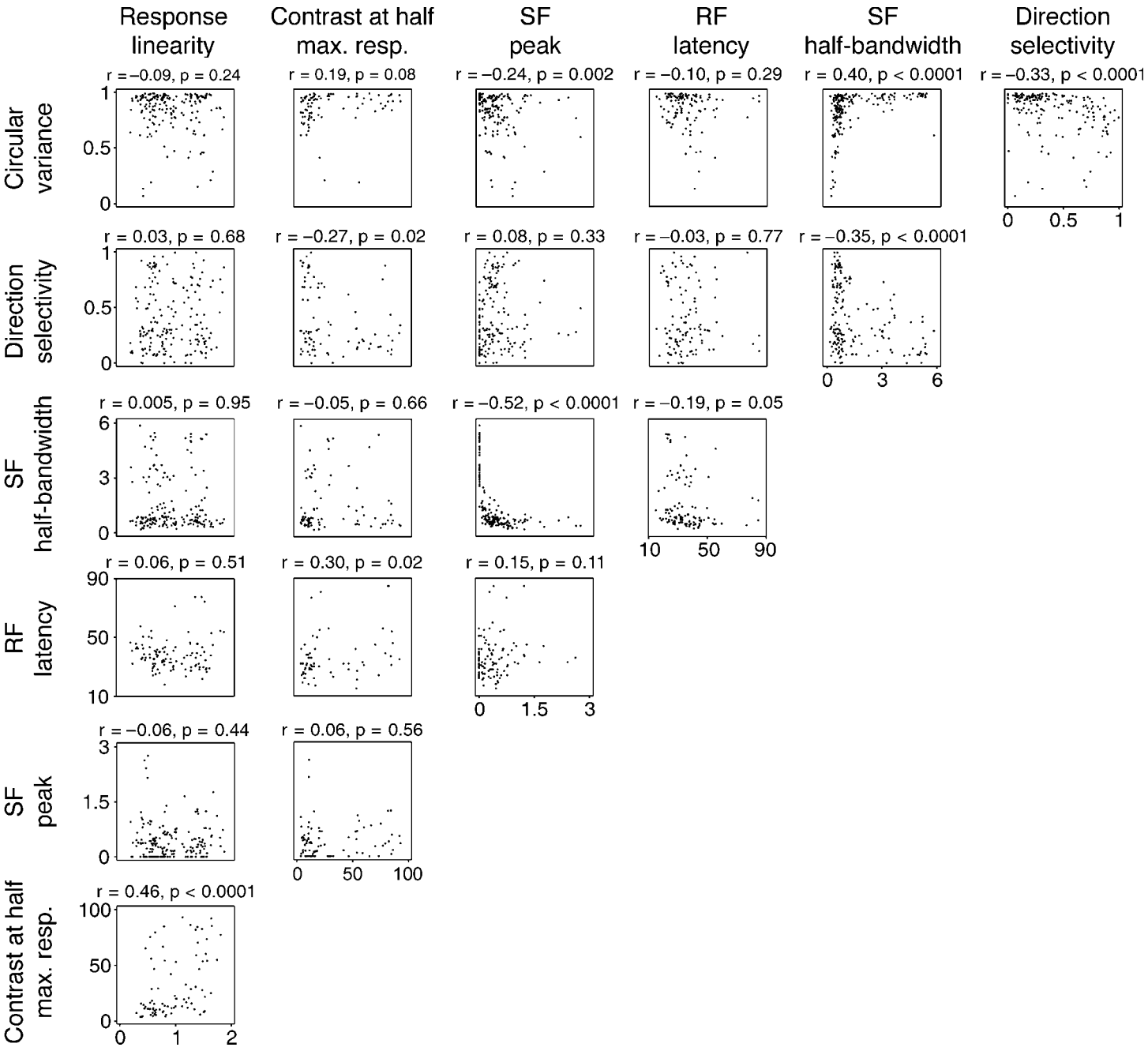

Figure 7. Linear correlations between different response properties. Scatter plots are shown for each pair combination. The correlation coefficient (*r*) and *p* values are shown at the top of each scatter plot.

five different methods (in addition to response linearity). These five methods quantify the subtraction between on and off regions (discreteness), their spatial correlation (correlation coefficient), the distance between their centers (normalized distance), their overlap (overlap index), and their relative phases (relative phase).

In spite of the differences in the mean spontaneous firing rate and size of the samples from our study and that of Mata and Ringach (2005), the measurements are remarkably similar (compare Figure 6 with Figure 3 of Mata & Ringach, 2005). The most similar correlations measured are the normalized distance versus correlation coefficient ($r = -0.41$ awake, $r = -0.41$ anesthetized), relative phase versus overlap index ($r = -0.74$ awake, $r = -0.72$ anesthetized), and relative phase versus normalized distance ($r = 0.40$ awake, $r = 0.43$ anesthetized). The most different correlations measured are the relative phase versus correlation coefficient ($r = -0.43$ awake, $r = -0.79$ anesthetized), the overlap index versus the correlation coefficient ($r = 0.58$ awake, $r = 0.93$ anesthetized), and the relative phase versus the discreteness ($r = 0.45$ awake, $r = 0.73$ anesthetized).

We also measured other basic response properties such as contrast sensitivity, spatial frequency peak/bandwidth, response latency, response linearity, direction selectivity, and circular variance (Figure 7). Although most of the correlations among these properties have not yet been measured in anesthetized primate, those that were measured are similar to the ones reported here for awake primates (e.g., circular variance with response linearity and spatial frequency bandwidth in Ringach, Shapley, et al., 2002).

Some of the correlations between basic response properties deserve to be discussed in further detail. For example, the correlations involving different combinations of circular variance, direction selectivity, spatial frequency bandwidth, and spatial frequency peak tended to have correlation coefficients greater than 0.3 and be highly significant. This finding indicates that neurons that are highly selective to a feature of the visual scene (e.g., orientation) tend to be highly selective to others (e.g., spatial frequency and/or direction of movement). For example, cells with the highest direction selectivity and sharpest orientation selectivity were also very selective in their spatial frequency tuning (SF bandwidth versus direction selectivity, $r = -0.35$, $p < 0.0001$; SF bandwidth versus circular variance, $r = 0.4$, $p < 0.0001$). Interestingly, the contrast that generated half-maximum response was not correlated to any response property except response linearity. However, the correlation with response linearity was quite strong ($r = 0.46$, $p < 0.0001$), which reveals a tendency for neurons that generate linear responses to be poorly sensitive to contrast.

Discussion

Our results demonstrate that response linearity is bimodally distributed in the awake primary visual cortex. This bimodal distribution was demonstrated in a cell sample with a median spontaneous firing rate that is ~6 times higher than that reported under anesthesia. In spite of this pronounced difference in mean spontaneous firing rate, we show that the basic response properties are similarly distributed and show similar correlations to those obtained in the anesthetized preparation. We also demonstrate that the spontaneous firing rate is correlated with the response selectivity and response latency to stimuli but not with other properties such as response linearity, spatial frequency tuning, contrast sensitivity, and receptive field structure.

While previous studies have clearly demonstrated that F1/F0 ratios are bimodally distributed in the anesthetized animal (De Valois et al., 1982; Dean & Tolhurst, 1983; Ibbotson et al., 2005; Mata & Ringach, 2005; Priebe et al., 2004; Ringach, Shapley, et al., 2002; Schiller et al., 1976b; Skottun et al., 1991), the number of studies that used the F1/F0 ratio as a criteria to classify cortical cells is much larger than the number of studies that have demonstrated a significant bimodal distribution (see Table 1). There are multiple examples of studies that measured the distribution of F1/F0 ratios and failed to find significance for bimodality as, for example, Mata and Ringach (2005) in anesthetized primate and Heimel, Van Hooser, and Nelson (2005) in anesthetized squirrel. In the awake primate, there are currently no published papers that demonstrate a bimodal distribution of F1/F0, and Kagan et al. (2002) reported a unimodal distribution. The reason for the inconsistency in finding a significant bimodal distribution for F1/F0 is unclear. One possibility is that the bimodality is relatively subtle and it can only be demonstrated with large data samples (Table 1). A second possibility is that the bimodality is strongly dependent on the stimulus conditions such as stimulus size, luminance contrast, and stimulus adaptation (Crowder, van Kleef, Dreher, & Ibbotson, 2007). A third possibility, suggested by our results, is that cells with different spatial frequency peaks for F1 and F0 (Figure 1c) blur the distribution of F1/F0 (when measurements are taken at only one spatial frequency). Yet a fourth possibility is that cells with high spontaneous firing rates shift the distribution toward the nonlinear side making it more unimodal (the distribution of F1/F0 was slightly shifted toward the linear side when the spontaneous firing rate was subtracted; Figure 2).

It has been recently proposed that the bimodal distribution of F1/F0 in the spike output could be the result of a nonlinear relationship between the membrane potential and the spike threshold (Mechler & Ringach, 2002; Priebe et al., 2004). Although a previous model proposed that response linearity was directly related to the distance between the resting membrane potential and the spike threshold (Chance et al., 1999), the measurements from Priebe et al. (2004) in cat visual cortex did not support this proposal. Our results are consistent with those from Priebe et al. by showing that response linearity and spontaneous firing rate are weakly correlated in awake V1. Previous studies in anesthetized animals have reported differences in spontaneous firing rates across cell types (Gilbert, 1977; Ringach, Shapley, et al., 2002; Schiller et al., 1976a). For example, Schiller et al. (1976a) and Ringach, Shapley, et al. (2002) found that the average spontaneous rate was significantly higher in complex cells than simple cells in the anesthetized primate. And in the anesthetized cat, Gilbert (1977) found that all cells with spontaneous firing rates >10 spikes/sec were complex cells. Our results are consistent with these previous studies by showing a weak tendency for cells that generate nonlinear responses to have a wider range of spontaneous firing rates than those that generate linear responses (Figure 3d).

Interestingly, our results demonstrate that the spontaneous firing rate is more closely related to the response selectivity to stimuli than response linearity. In particular, the values of spontaneous firing rate and circular variance were found to be constrained to a triangular relation so that cells with the highest spontaneous activity had low

orientation selectivity and those with the sharpest orientation tuning had low spontaneous firing rates. Similar triangular relationships between spontaneous firing rate and circular variance were previously demonstrated in the anesthetized primate (Ringach, Shapley, et al., 2002; Xing et al., 2004) in a sample with considerably lower spontaneous firing rates. The lower spontaneous firing rate in previous studies is likely to reflect the effect of anesthesia; however, we cannot discard a possible difference in sampling (e.g., different eccentricities, electrode bias). The relation between spontaneous firing rate and response selectivity is consistent with models that propose a major role for intracortical inhibition in sharpening orientation tuning (McLaughlin, Shapley, Shelley, & Wielaard, 2000; Ringach, Bredfeldt, Shapley, & Hawken, 2002; Ringach, Hawken, & Shapley, 1997; Troyer, Krukowski, Priebe, & Miller, 1998).

In summary, our results are consistent with the notion that response linearity is determined by the nonlinear relation between the membrane potential and the spike threshold (Chance et al., 1999; Mechler & Ringach, 2002; Priebe et al., 2004). Importantly, we show that this mechanism is likely to operate similarly in the anesthetized and awake brains. Given that neuronal excitability can greatly vary with behavioral state (Bezdudnaya et al., 2006; Cano, Bezdudnaya, Swadlow, & Alonso, 2006), it could be possible that the distribution of response linearity was also state dependent. This possibility was supported by the lack of consistency in reporting bimodal distributions of F1/F0 ratios (Table 1) and the lack of proof that response linearity was bimodally distributed in the awake brain.

The use of response linearity to classify cortical cells has clear theoretical advantages; however, it should be noted that the response linearity is just one response parameter that differs among cortical neurons. Whereas the number of identified retinal ganglion cells has been increasing over the years (Masland, 2004), the diverse anatomical cell types within the cerebral cortex are still been lumped into only two types: linear and nonlinear. A major goal of visual neuroscience should be to discover the critical parameters that distinguish the different cell types in the different layers of the visual cortex (Williams & Shapley, 2007).

Conclusions

We demonstrated that response linearity is bimodally distributed in V1 neurons of the awake brain. Although our cell sample in the awake brain has a median spontaneous firing rate ~6 times higher than in the anesthetized V1, the statistics of the basic response properties (distributions and correlations) are remarkably similar to those reported under anesthesia. The spontaneous rate is significantly correlated with the orientation selectivity of the cell but not with other properties such as the response linearity, spatial frequency tuning, contrast sensitivity, and receptive field structure. Our results are consistent with the notion that general anesthesia reduces cortical excitability without altering basic neuronal response properties and support models that associate an increase in neuronal excitability with a reduction in response selectivity to stimuli.

Acknowledgments

We would like to thank Nadia Gamez Gomez and Javier Cubo Villalba for helping in the development of analysis software. We would also like to thank Barry Lee and Qasim Zaidi for their comments on an earlier version of this manuscript. The research was supported by NIH-EY 14345, NIH-NS 059753, and The Research Foundation at the State University of New York.

Commercial relationships: none.
Corresponding author: Jose-Manuel Alonso.
Email: jalonso@sunyopt.edu.
Address: 33 West 42nd Street, New York, NY 10036, USA.

References

Ben-Yishai, R., Bar-Or, R. L., & Sompolinsky, H. (1995). Theory of orientation tuning in visual cortex. *Proceedings of the National Academy of Sciences of the United States of America, 92,* 3844–3848. [PubMed] [Article]

Bezdudnaya, T., Cano, M., Bereshpolova, Y., Stoelzel, C. R., Alonso, J. M., & Swadlow, H. A. (2006). Thalamic burst mode and inattention in the awake LGNd. *Neuron, 49,* 421–432. [PubMed]

Cano, M., Bezdudnaya, T., Swadlow, H. A., & Alonso, J. M. (2006). Brain state and contrast sensitivity in the awake visual thalamus. *Nature Neuroscience, 9,* 1240–1242. [PubMed]

Casanova, C., Nordmann, J. P., Ohzawa, I., & Freeman, R. D. (1992). Direction selectivity of cells in the cat's striate cortex: Differences between bar and grating stimuli. *Visual Neuroscience, 9,* 505–513. [PubMed]

Chance, F. S., Nelson, S. B., & Abbott, L. F. (1999). Complex cells as cortically amplified simple cells. *Nature Neuroscience, 2,* 277–282. [PubMed]

Chino, Y. M., Smith, E. L., 3rd, Yoshida, K., Cheng, H., & Hamamoto, J. (1994). Binocular interactions in striate cortical neurons of cats reared with discordant visual inputs. *Journal of Neuroscience, 14,* 5050–5067. [PubMed]

Conway, B. R., & Livingstone, M. S. (2003). Space-time maps and two-bar interactions of different classes of direction-selective cells in macaque V-1. *Journal of Neurophysiology, 89,* 2726–2742. [PubMed] [Article]

Crowder, N. A., van Kleef, J., Dreher, B., & Ibbotson, M. R. (2007). Complex cells increase their phase sensitivity at low contrasts and following adaptation. *Journal of Neurophysiology, 98,* 1155–1166. [PubMed] [Article]

Cumming, B. G., Thomas, O. M., Parker, A. J., & Hawken, M. J. (1999). Classification of simple and complex cells in V1 of the awake monkey. *Society for Neuroscience Abstracts, 25,* 1548.

De Valois, R. L., Albrecht, D. G., & Thorell, L. G. (1982). Spatial frequency selectivity of cells in macaque visual cortex. *Vision Research, 22,* 545–559. [PubMed]

Dean, A. F. (1981). The relationship between response amplitude and contrast for cat striate cortical neurones. *The Journal of Physiology, 318,* 413–427. [PubMed] [Article]

Dean, A. F., & Tolhurst, D. J. (1983). On the distinctness of simple and complex cells in the visual cortex of the cat. *The Journal of Physiology, 344,* 305–325. [PubMed] [Article]

DeAngelis, G. C., Freeman, R. D., & Ohzawa, I. (1994). Length and width tuning of neurons in the cat's primary visual cortex. *Journal of Neurophysiology, 71,* 347–374. [PubMed]

Dougherty, P. M., Li, Y. J., Lenz, F. A., Rowland, L., & Mittman, S. (1997). Correlation of effects of general anesthetics on somatosensory neurons in the primate thalamus and cortical EEG power. *Journal of Neurophysiology, 77,* 1375–1392. [PubMed] [Article]

Douglas, R. J., Koch, C., Mahowald, M., Martin, K. A., & Suarez, H. H. (1995). Recurrent excitation in neocortical circuits. *Science, 269,* 981–985. [PubMed]

Ferster, D., & Lindstrom, S. (1983). An intracellular analysis of geniculo-cortical connectivity in area 17 of the cat. *The Journal of Physiology, 342,* 181–215. [PubMed] [Article]

Gilbert, C. D. (1977). Laminar differences in receptive field properties of cells in cat primary visual cortex. *The Journal of Physiology, 268,* 391–421. [PubMed] [Article]

Hartigan, J. A., & Hartigan, P. M. (1985). The dip test of unimodality. *Annals of Statistics, 13,* 70–84.

Hawken, M. J., Shapley, R. M., & Grosof, D. H. (1996). Temporal-frequency selectivity in monkey visual cortex. *Visual Neuroscience, 13,* 477–492. [PubMed]

Heimel, J. A., Van Hooser, S. D., & Nelson, S. B. (2005). Laminar organization of response properties in primary visual cortex of the gray squirrel (Sciurus carolinensis). *Journal of Neurophysiology, 94,* 3538–3554. [PubMed] [Article]

Hirsch, J. A., Martinez, L. M., Alonso, J. M., Desai, K., Pillai, C., & Pierre, C. (2002). Synaptic physiology of the flow of information in the cat's visual cortex in vivo. *The Journal of Physiology, 540,* 335–350. [PubMed] [Article]

Hubel, D. H., & Wiesel, T. N. (1962). Receptive fields, binocular interaction and functional architecture in the cat's visual cortex. *The Journal of Physiology, 160,* 106–154. [PubMed] [Article]

Hubel, D. H., & Wiesel, T. N. (1968). Receptive fields and functional architecture of monkey striate cortex. *The Journal of Physiology, 195,* 215–243. [PubMed] [Article]

Ibbotson, M. R., Price, N. S., & Crowder, N. A. (2005). On the division of cortical cells into simple and complex types: A comparative viewpoint. *Journal of Neurophysiology, 93,* 3699–3702. [PubMed] [Article]

Jones, J. P., & Palmer, L. A. (1987). The two-dimensional spatial structure of simple receptive fields in cat striate cortex. *Journal of Neurophysiology, 58,* 1187–1211. [PubMed]

Kagan, I., Gur, M., & Snodderly, D. M. (2002). Spatial organization of receptive fields of V1 neurons of alert monkeys: Comparison with responses to gratings. *Journal of Neurophysiology, 88,* 2557–2574. [PubMed] [Article]

Lennie, P., Krauskopf, J., & Sclar, G. (1990). Chromatic mechanisms in striate cortex of macaque. *Journal of Neuroscience, 10,* 649–669. [PubMed] [Article]

Masland, R. H. (2004). Neuronal cell types. *Current Biology, 14,* R497–R500. [PubMed]

Mata, M. L., & Ringach, D. L. (2005). Spatial overlap of ON and OFF subregions and its relation to response modulation ratio in macaque primary visual cortex. *Journal of Neurophysiology, 93,* 919–928. [PubMed] [Article]

McLaughlin, D., Shapley, R., Shelley, M., & Wielaard, D. J. (2000). A neuronal network model of macaque primary visual cortex (V1): Orientation selectivity and dynamics in the input layer 4Calpha. *Proceedings of the National Academy of Sciences of the United States of America, 97,* 8087–8092. [PubMed] [Article]

Mechler, F., & Ringach, D. L. (2002). On the classification of simple and complex cells. *Vision Research, 42,* 1017–1033. [PubMed]

Movshon, J. A., Thompson, I. D., & Tolhurst, D. J. (1978a). Receptive field organization of complex cells in the cat's striate cortex. *The Journal of Physiology, 283,* 79–99. [PubMed] [Article]

Movshon, J. A., Thompson, I. D., & Tolhurst, D. J. (1978b). Spatial summation in the receptive fields of simple cells in the cat's striate cortex. *The Journal of Physiology, 283,* 53–77. [PubMed] [Article]

Ohzawa, I., DeAngelis, G. C., & Freeman, R. D. (1996). Encoding of binocular disparity by simple cells in the cat's visual cortex. *Journal of Neurophysiology, 75,* 1779–1805. [PubMed]

Ohzawa, I., DeAngelis, G. C., & Freeman, R. D. (1997). Encoding of binocular disparity by complex cells in the cat's visual cortex. *Journal of Neurophysiology, 77,* 2879–2909. [PubMed] [Article]

Priebe, N. J., Mechler, F., Carandini, M., & Ferster, D. (2004). The contribution of spike threshold to the dichotomy of cortical simple and complex cells. *Nature Neuroscience, 7,* 1113–1122. [PubMed]

Ringach, D. L., Bredfeldt, C. E., Shapley, R. M., & Hawken, M. J. (2002). Suppression of neural responses to nonoptimal stimuli correlates with tuning selectivity in macaque V1. *Journal of Neurophysiology, 87,* 1018–1027. [PubMed] [Article]

Ringach, D. L., Hawken, M. J., & Shapley, R. (1997). Dynamics of orientation tuning in macaque primary visual cortex. *Nature, 387,* 281–284. [PubMed]

Ringach, D. L., Shapley, R. M., & Hawken, M. J. (2002). Orientation selectivity in macaque V1: Diversity and laminar dependence. *Journal of Neuroscience, 22,* 5639–5651. [PubMed] [Article]

Sceniak, M. P., Ringach, D. L., Hawken, M. J., & Shapley, R. (1999). Contrast's effect on spatial summation by macaque V1 neurons. *Nature Neuroscience, 2,* 733–739. [PubMed]

Schiller, P. H., Finlay, B. L., & Volman, S. F. (1976a). Quantitative studies of single-cell properties in monkey striate cortex: I. Spatiotemporal organization of receptive fields. *Journal of Neurophysiology, 39,* 1288–1319. [PubMed]

Schiller, P. H., Finlay, B. L., & Volman, S. F. (1976b). Quantitative studies of single-cell properties in monkey striate cortex: III. Spatial frequency. *Journal of Neurophysiology, 39,* 1334–1351. [PubMed]

Skottun, B. C., Bradley, A., Sclar, G., Ohzawa, I., & Freeman, R. D. (1987). The effects of contrast on visual orientation and spatial frequency discrimination: A comparison of single cells and behavior. *Journal of Neurophysiology, 57,* 773–786. [PubMed]

Skottun, B. C., De Valois, R. L., Grosof, D. H., Movshon, J. A., Albrecht, D. G., & Bonds, A. B. (1991). Classifying simple and complex cells on the basis of response modulation. *Vision Research, 31,* 1079–1086. [PubMed]

Skottun, B. C., & Freeman, R. D. (1984). Stimulus specificity of binocular cells in the cat's visual cortex: Ocular dominance and the matching of left and right eyes. *Experimental Brain Research, 56,* 206–216. [PubMed]

Skottun, B. C., Grosof, D. H., & De Valois, R. L. (1988). Responses of simple and complex cells to random dot patterns: A quantitative comparison. *Journal of Neurophysiology, 59,* 1719–1735. [PubMed]

Smith, E. L., 3rd, Chino, Y. M., Ni, J., Ridder, W. H., 3rd, & Crawford, M. L. (1997). Binocular spatial phase tuning characteristics of neurons in the macaque striate cortex. *Journal of Neurophysiology, 78,* 351–365. [PubMed] [Article]

Somers, D. C., Nelson, S. B., & Sur, M. (1995). An emergent model of orientation selectivity in cat visual cortical simple cells. *Journal of Neuroscience, 15,* 5448–5465. [PubMed]

Swadlow, H. A., Bereshpolova, Y., Bezdudnaya, T., Cano, M., & Stoelzel, C. R. (2005). A multi-channel, implantable microdrive system for use with sharp, ultra-fine "Reitboeck" microelectrodes. *Journal of Neurophysiology, 93,* 2959–2965. [PubMed] [Article]

Troyer, T. W., Krukowski, A. E., Priebe, N. J., & Miller, K. D. (1998). Contrast-invariant orientation tuning in cat visual cortex: Thalamocortical input tuning and correlation-based intracortical connectivity. *Journal of Neuroscience, 18,* 5908–5927. [PubMed] [Article]

Williams, P. E., & Shapley, R. M. (2007). A dynamic nonlinearity and spatial phase specificity in macaque V1 neurons. *Journal of Neuroscience, 27,* 5706–5718. [PubMed] [Article]

Xing, D., Ringach, D. L., Shapley, R., & Hawken, M. J. (2004). Correlation of local and global orientation and spatial frequency tuning in macaque V1. *The Journal of Physiology, 557,* 923–933. [PubMed] [Article]

Zurita, P., Villa, A. E., de Ribaupierre, Y., de Ribaupierre, F., & Rouiller, E. M. (1994). Changes of single unit activity in the cat's auditory thalamus and cortex associated to different anesthetic conditions. *Neuroscience Research, 19,* 303–316. [PubMed]